

Interactive comment on “Fluid-mediated, brittle-ductile deformation at seismogenic depth: Part I – Fluid record and deformation history of fault-veins in a nuclear waste repository (Olkiluoto Island, Finland)” by Barbara Marchesini et al.

Barbara Marchesini et al.

barbara.marchesini2@unibo.it

Received and published: 2 April 2019

394 Reviewer: The ranges in these fluid inclusion values is too large to be interpretable. See general comments above.

Authors: We repeat in her the comment we posted to the other Reviewer, Prof. Olivier Vanderhaeghe, who wrote: “The homogenization temperatures and salinities obtained on the analysis of what is presented as a consistent assemblage of fluid inclusions display rather wide ranges of values”. We give here a detailed discussion of this issue

C1

in order to critically consider the degree to which our dataset is interpretable in light of the current knowledge. A comparison between the 0-5 wt% NaCleq salinity range reported in our manuscript and that of typical crustal reservoirs is useful on this regard. Figures 1 and 2 presented in reported in Yardley & Graham 2002 show a number of such reservoirs, namely sedimentary and metamorphic fluids from shallow marine basins and continental margin rocks, from which is clear that the estimated 0-5 wt% NaCleq salinity range is not too large as claimed. The salinity-temperature ranges that mark the 1-31 boxes of Fig. 2 of identify fluids from some large reservoirs, like those of the sediments above the Salt Dome Basin of the Mississippi (box 5) and fluids from the Southern and Central North Sea formation waters (boxes 6 and 7, respectively). These fluids were generated in geological environments that cannot be compared with Olkiluoto, and their salinities were determined with techniques that were distinct from those we used here. However, the boxes 16, 18, 19, 20, 25, and 28 of Fig. 2 of Yardley & Graham consistently identify syn- to post-metamorphic fluids from quartz veins that were studied with fluid inclusion microanalysis. These fluids can be directly compared with our dataset. It is clear that the fluids that formed the veins within the Waterville Fm. metasediments (box 19) and the veins of the Connemara schists of Ireland (box 25) show bulk salinities that are comparable with the BFZ300 fluid. The others have ranges that are actually larger than that of the BFZ300. Hence, the salinity range determined at Olkiluoto cannot be considered large. In terms of textbook classification (e.g., Pirajno, 2009), the fluids sealed within the FIAs of the BFZ300 can be classified as low-salinity fluids, and their range is comparable to that documented in several metamorphic veins from a large number of geological environments. From Fig. 1 of Yardley & Graham it can be seen that fluids similar to those of Olkiluoto formed the veins of the Shimanto accretionary complex of Japan, the veins of the Otago schists and Torlesse metasediments of New Zealand, and the veins in the Hill End Goldfield of New South Wales-Australia (boxes 11, 13, 14, 33, 15, respectively). In the new version of the manuscript, we will make a comparison between the fluid data reviewed by Yardley & Graham and those of the BFZ300, in order to emphasize this aspect. It is

C2

important to stress that although several events of fluid entrapment occurred within the BFZ300, they did not necessarily correspond to sealing of exactly the same batch of fluid. Several generations of distinct – but all low-salinity – fluids must have been injected into the fault and formed the quartz-chlorite assemblage, as suggested by distinct chlorite compositions and textures (see supplementary figure). Regarding the ranges of T_{tot} measured in the FIAs: we show that the 150-200 °C ranges measured in individual FIAs of the BFZ300 can be explained by an effect of re-equilibration during post-entrapment deformation. The T_{tot} histograms lack specific modes (line 487 of manuscript) and no statistical data including mean, range, standard deviation, extreme values, etc. could be used to evaluate the regime of post-entrapment deformation. This makes the application of the interpretation criteria of the relevant literature (see reply to comment 190) difficult to apply. Our suggestion whereby the 1-5 wt% Na-Cleq fluid inclusions homogenizing in the 200-350 °C interval reflect the characteristic properties of the vast majority of damage zone and of the fault core fluids is coherent with the established notion that a number of inclusions survive virtually intact the modified post-entrapment PT conditions (Diamond et al., 2010; Vityk and Bodnar, 1998). This range is in line with the temperature ranges estimated with the quartz-chlorite and sphalerite-stannite geothermometers. Thus, the strength of this dataset is the number of concurrent geothermometric data, rather than the rigorous validity of the T_{tot} histograms. Thus, the strength of this dataset is the number of concurrent geothermometric data, rather than the rigorous validity of the T_{tot} histograms. We note that similar re-equilibration effects have been recorded also in the orogenic Au-veins (see discussion in: Garofalo et al., 2014), for which the fault-valve model of Sibson et al. was proposed (Sibson et al., 1988).

458 Reviewer: Based on your histograms I can't evaluate this statement. Histograms are not informative representations of fluid inclusion data. Box and whisker plots are preferred. For instance, you could plot salinity and T_h for each FIA next to each other so that we can check if T_h and salinity ranges somehow correlate. As shown, there could be many reasons for these wide data spreads: Mix-up of FIAs that formed under

C3

widely varying conditions (perhaps most likely); partial resetting or necking (although difficult to explain the T_m ranges); partial leakage during freezing (would explain range in T_m but be visible during freezing run); or a combination of all these. Which inclusions are primary, which secondary?

Authors: Because the reviewer suggests using the paper by Fall & Bodnar (2018) as a benchmark for our study, we reckon he/she suggests plotting our data like the box and whiskers plots of Figs 4-9, 15, and 20 of Fall & Bodnar. We find these plots extremely useful; however, we think they would not be effective in our study. Box plots are very efficient when large datasets from tens of FIAs must be compared with each other, which is the case of Fall & Bodnar's study; however, they do not work well when microthermometry data from individual natural and synthetic FIAs need to be compared. In their Fig. 16, Fall & Bodnar use actually histograms to show the effects of post-entrapment re-equilibration in an individual FIA from an orogenic Au deposit by making a direct comparison with a re-equilibrated synthetic FIA. In our work we followed the same approach by plotting the histograms of Fig. 10 (recording the minimum and maximum T_{mice} and T_{tot} for each assemblage) and making comparisons with the literature data on synthetic FIAs. Thus, histograms are useful in our case. The reviewer claims that there could be many reasons for the wide data spreads of the studied FIAs, one of which would be a supposed mix-up of FIAs. This possibility can be excluded by the fact that the petrographic work carried out before microthermometry is used to map (see supplementary material) and record each inclusion of a FIAs before microthermometry starts. Regarding the primary and secondary FIAs: we have shown that the studied quartz crystals are characterized by a complex network of healed cracks and, indeed, also by many FIAs arranged as trails, cross-cutting and superimposed on each other and apparently arranged in clusters. Hence, we could not confidently identify any primary undeformed fluid inclusions. We only identified a few clusters of primary fluid inclusions within Qtz II (line 382), but they showed irregular and decrepitated morphologies. Thus, microthermometric determinations were not possible in those inclusions and we decided to not emphasize their presence. Secondary

C4

and pseudosecondary FIAs are reported in Fig. 10 with the acronyms Type S1, Type S2, Type S4, and Type PS, respectively. Regarding the bivariate Thtot-salinity plots: as suggested by the reviewer we prepared a single diagram where we reported all the microthermometric datapoints divided for structural domains, in accordance with the scheme we proposed in the manuscript (please, see supplementary material). This new plot is of difficult interpretation, also in the light that our FIAs were subjected to post-entrapment modifications as clearly highlighted by frequency diagrams reported in the manuscript. Moreover, the proposed plot, it excludes fluid mixing within the FIAs based on the scatter of the data. Indeed, the Thtot and the calculated salinities of all the FIAs from BFZ300 plot within large ranges of the diagram and overlap with each other, suggesting that there is no systematic co-variation of the fluid properties that was caused by clear distinct fluids or fluid mixing. The co-variations or correlations mentioned by the reviewer are therefore not clear evident in our samples. However, they are evident in Fig. 3 of Fall & Bodnar, which makes this type of plot for 20 FIAs entrapped within a sphalerite crystal from a vein of the well-known epithermal Zn-Ag-Pb deposit of Creede, Colorado (1: oldest FIA; 20: youngest FIA). It is clear that the 20 FIAs entrapped within the Creede sphalerite define very tight Thtot-salinity intervals, which differ from each other and form a trend starting from a high salinity/high T “end member” fluid (Thtot: 260-270 °C; Salinity: 9-11 wt% NaCleq) and ending with a low salinity/low T end member (Thtot: 200-220 °C; Salinity: 6 wt% NaCleq). Such trend can be explained – at the scale of a single crystal – by progressive mixing of the two end-member fluids that generated the 20 FIAs at progressively later stages of entrapment. All these features are completely missing in the Olkiluoto FIA dataset.

Interactive comment on Solid Earth Discuss., <https://doi.org/10.5194/se-2019-5>, 2019.

C5

Yardley & Graham (2002)

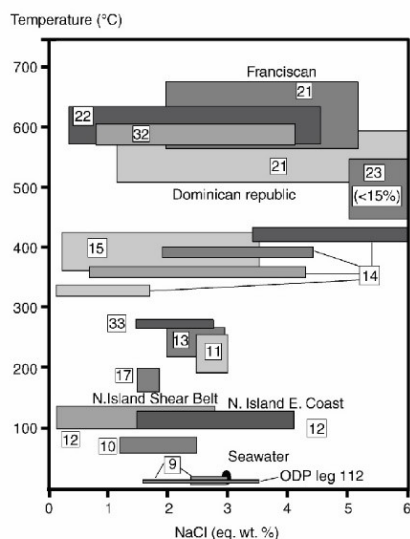


Fig. 1. Temperature-salinity plot for formation waters, spring waters and metamorphic fluids hosted by sequences of oceanic or accretionary prism origin. Boxes reflect the range of data from each of the numbered sources detailed in Table 1. Note the different horizontal scale to that of Fig. 2.

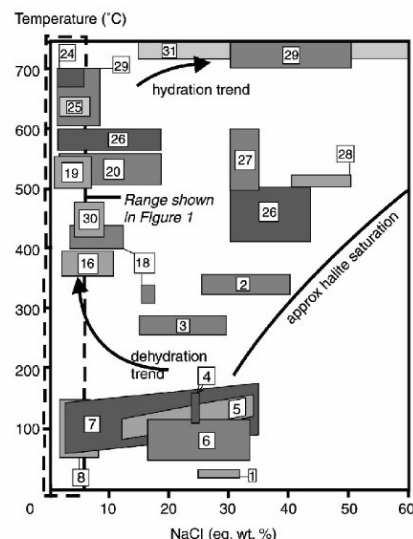


Fig. 2. Temperature-salinity plot for formation waters and metamorphic fluids hosted by sequences deposited in shallow seas and at continental margins. Boxes reflect the range of data from each of the numbered sources detailed in Table 1. The dashed box encloses the more restricted range of conditions plotted in Fig. 1.

Fig. 1. From Yardley and Graham (2002). Please, refer to the main comment for expanded discussion.

C6

Fall & Bodnar (2018), Fig. 3

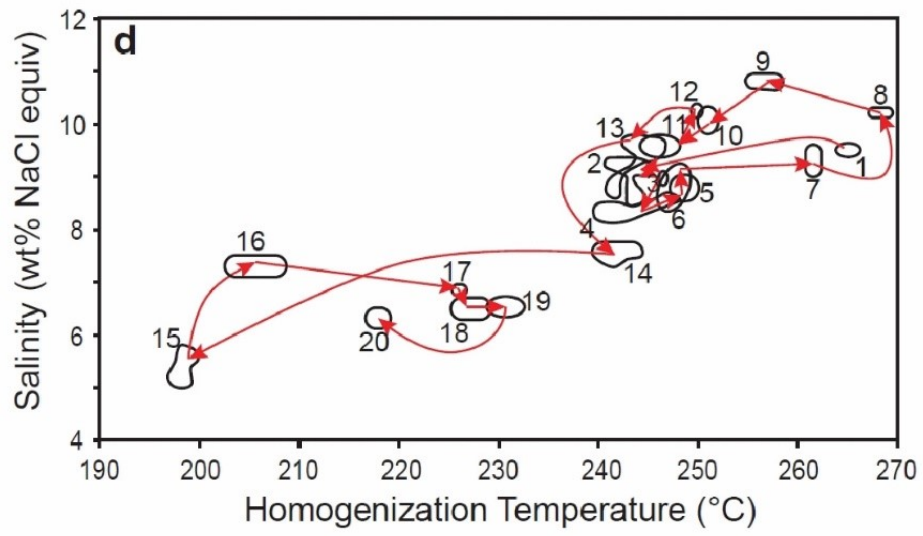


Fig. 2. From Fall and Bodnar (2018). Please, refer to the main text.